Earth, Planets and Space

EXPRESS LETTER

Open Access

Estimation of emission mass from an eruption plume for the Aso volcano eruption, on October 8, 2016, using a four-dimensional variational method

Kensuke Ishii*

Abstract

When an explosive eruption, such as a Plinian eruption, occurs, in order to estimate ash fall around the volcano and for hazard mitigation, a numerical model is often used. Simulation by a numerical model needs emission mass from the eruption column including vertical profile and size distribution of ash particles. Hence, the accuracy of the emission mass from the eruption column is vital to estimate and forecast ash fall accurately. We developed a data assimilation system based on the four-dimensional variational method (4D-Var) as an estimation method for emission mass from volcanic eruption columns as a function of altitude and ash particle size. This system includes a forward model which calculates volcanic ash forecast, and an observation operator, which are used for the calculation of misfit between observation and forecast. It also includes an adjoint model of the forward model which calculates the correction of emission mass from the misfit, and an algorithm to minimize the cost function as a measurement of optimization. In this system, observation and prior knowledge about emission mass from the volcanic eruption column, such as the Suzuki function, can be simultaneously treated with weight considering observation error and background error. Furthermore, this system has scalability for additional observations. That is to say, a variety of observations can be treated simultaneously, only if their observation operators which are an transformation from model parameters to observation value are developed. In this study, we applied this system to the October 8, 2016 Aso volcano eruption in Japan. After this eruption, ash fall observation (including lapilli) around Aso volcano was preformed, and operational weather radar captured the eruption cloud echo. Using both of these observations and the 4D-Var system, we estimated emission mass from the eruption plume column as a function of altitude and particle size, and it led to ash fall simulation which was consistent with observations. In addition, the eruption mass which is the sum of emission mass from eruption column was estimated to be 1.32×10^8 kg.

Keywords: Data assimilation, Four-dimensional variational method, 4D-Var, Atmospheric transport model, Aso volcano

Introduction

When an eruption occurs, we need to know about eruption source parameters such as eruption mass, height of the eruption column and duration of the eruption to forecast next possible hazards for mitigation. Although ash fall from explosive eruptions does not always take human life directly, even a minor ash fall impacts human health, farming lifelines and aviation safety (Mannen 2014; Klawonn et al. 2012). In general, ash fall forecast is calculated by numerical models which need emission mass as an initial distribution (i.e. mass of ash and lapilli particle segregation from the eruption column) of volcanic ash including ash particle size and ash amount depending on altitude (e.g. Bonadonna et al. 2005), and the accuracy of ash fall simulation is particularly constrained by the difficulty of quantifying the ESPs

*Correspondence: kishii@mri-jma.go.jp
Volcanology Research Department, Meteorological Research Institute, 1-1 Nagamine, Tsukuba, Ibaraki 305-0052, Japan

(eruption source parameters) as initial distribution (e.g. Folch 2012). Some ash fall simulations use empirical and theoretical assumptions such as the Suzuki function for the initial distribution of volcanic ash. In the Suzuki function, the total size distribution of ash particles is assumed as log-normal distribution, and the emission mass for each particle size and each altitude is calculated by a simplified model of vertical velocity of an eruption column and terminal velocity (e.g. Shimbori et al. 2010; Folch 2012). However, the reliability of such distribution has yet to be verified in detail. For verification of empirical distribution and understanding of the nature of an eruption column, reconstruction of the ash particle segregation pattern along the eruption column from observation using an inversion method is key (Mannen 2014). There are a variety of inversion methods in diverse fields such as weather forecasts (e.g. Kalnay 2002). Of these, the four-dimensional variational method (4D-Var) is one of the most sophisticated data assimilation methods and widely used in weather forecasts of meteorological organizations of various countries (e.g. WMO 2001). 4D-Var is an optimization method based on Bayesian statistics. In 4D-Var, prior information and observation can be simultaneously considered. In addition, in the 4D-Var, because a variety of observations such as ash fall observation and radar observation are simultaneously possible, there is a possibility that diverse of information such as size distribution and the time series of emission can be extracted by combining them with model dynamics.

In this study, we developed a data assimilation system based on 4D-Var for the estimation of emission mass from an eruption plume as a function of altitude and ash particle size, and we applied it to the case of the 2016 Aso volcano eruption in Japan. We obtained an initial distribution of ash particles which led to a forecast that was consistent with ash fall observation.

Data assimilation methodology

Overview of the 4D-Var system for volcanic ash

We analyse emission mass from an eruption plume by 4D-Var. This method is an optimization method based on Bayesian statistics (e.g. Kalnay 2002). The optimization is to find certain variables (called "analysis variables") minimizing a cost function J, including a term of difference between forecast and the background, the difference between forecast and observation, and a penalty term. In this study, the cost function J is defined as follows

$$J[\tilde{\mathbf{x}}(t_1),\ldots,\tilde{\mathbf{x}}(t_N)] = \frac{1}{2}\sum_{i=1}^{N}\left[\tilde{\mathbf{x}}(t_i)-\tilde{\mathbf{x}}_{\boldsymbol{g}}(t_i)\right]^{\mathrm{T}}\mathbf{B}^{-1}\left[\tilde{\mathbf{x}}(t_i)-\tilde{\mathbf{x}}_{\boldsymbol{g}}(t_i)\right]+\frac{1}{2}\sum_{j=1}^{K}\left[\boldsymbol{H}(\mathbf{x}(t_j))-\boldsymbol{y}_j\right]^{\mathrm{T}}\mathbf{R}^{-1}\left[\boldsymbol{H}(\mathbf{x}(t_j))-\boldsymbol{y}_j\right]+J_{\mathrm{p}}$$

where $\tilde{\mathbf{x}}(t_i)$ is the emission mass from the eruption column for a discretized diameter D_n and a discretized altitude z_k at a discretized time t_i

$$\tilde{\mathbf{x}}(t_i) = \mathbf{c}(z_k, D_n, t_i) \quad i = 1,\ldots,N$$

where $\mathbf{c}$ is the emission mass of volcanic ash (g/m^3) and N is the index of eruption duration (i.e. t_1 is the start time of the eruption, and t_N is the end time of the eruption). $\mathbf{x}(t_j)$ is the forecast value of ash concentration in the atmosphere and the ash fall amount (including lapilli) which are both functions of location and ash diameter. The forecast variable $\mathbf{x}(t_j)$ is calculated by a forward model $\boldsymbol{M}_t$ (atmospheric transport model) from emission mass $\tilde{\mathbf{x}}$, i.e. $\mathbf{x}(t_j) = \boldsymbol{M}_{t_j}(\tilde{\mathbf{x}})$. $\tilde{\mathbf{x}}_{\boldsymbol{g}}$ is the first guess which is based on prior information. For example, emission mass $\tilde{\mathbf{x}}_{\boldsymbol{g}}$ for each altitude and each particle diameter is reproduced by plume height in Suzuki (1983). $\mathbf{B}$ is the background error covariance which has characteristics of a model forecast error. $\boldsymbol{y}_j$ is defined as observation at time $t_j (j = 1,\ldots,K$. t_K is the end time of the data assimilation window). $\boldsymbol{H}$ is the observation operator which is a transformation from the model variable $\mathbf{x}(t_j)$ to observation value $\boldsymbol{y}_j$. For ash fall amount (g/m^2), the observation operator is the sum of each size of ash fall amount with a diameter of 2 mm or less, and it includes interpolation to the location of ash fall observation from the model grid.

J_{p} is a penalty term which has the effect to add constraints to the optimization of the variational data assimilation system (Parrish and Derber 1992). In this case, the emission mass for any size particle and any altitude must be positive, i.e. we take the penalty term J_{p} as follows

$$J_p = \mu\sum_{\mathrm{i}=1}^{N}\mathbf{x}(t_i)^2 \quad \text{for } \mathbf{x}(t_i) < 0 \text{ (g/m}^3\text{)}$$

where μ is the penalty term factor. This penalty term has the effect of increasing cost function J for negative emission mass. A sufficiently large μ restricts the optimization of the 4D-Var system with positive emission mass.

Description of forward model

The 4D-Var system includes a forward model $\boldsymbol{M}_t$ which calculates ash concentration and ash fall at the surface from emission mass $\tilde{\mathbf{x}}(t_i)$ from the eruption plume.

The model $\boldsymbol{M}_t$ is a Euler model using finite difference methods to calculate time evolution of volcanic ash concentration using dynamical processes such as advection

and gravity settling. For time discretization, the Euler scheme (e.g. Kalnay 2002) is used. For space discretization, we adopt a finite-volume method (FVM) which calculates the time evolution of volcanic ash concentration from flux of the grid boundaries. The forecast variables are volcanic ash concentration and ash fall. The volcanic ash concentration is defined as a function of each grid for each ash particle diameter, i.e. the number of forecast variables in one grid is the number of particle diameters. Ash fall forecast at the surface is also a forecast variable. For the advection process, we adopted third-order upwind discretization (Wicker and Skamarock 2002) and a flux limiter function (Koren 1993). The meteorological field, including wind, temperature and pressure, used in the advection process and gravitational process with interpolation linearly by space and time is the Meso Analysis. The Meso Analysis is a 3+1-dimensional (space and time) meteorological field, such as wind and temperature calculated by the Japan Meteorological Agency (JMA 2013) with approximately 5-km resolution horizontally for daily weather forecasts and meteorological hazard mitigation. The spatial coordinates are uniform for latitude, longitude and altitude. Gravitational settling is vertically downward advection calculated from terminal velocity which depends on the diameter of ash particles based on Shimbori et al. (2010). In the calculation of terminal velocity, particle density is based on Wilson and Huang (1979). In addition, diameter D of ash particles is defined as the mean of diameter of the major axis a_1 and short diameter $a_2 = a_3$ with a shape factor $\frac{a_2}{a_1} = \frac{1}{3}$ (Shimbori 2015). In this study, ash particle diameter D is defined by $D = \frac{1}{3}(a_1 + a_2 + a_3)$.

Optimization algorithm

The 4D-Var system calculates an optimized value (called the "analysis value") from a first guess by minimizing the cost function. For minimizing the cost function, we use an iteration method using the gradient of the cost function $\nabla_{\mathrm{i}} J = \partial J / \partial \tilde{\mathbf{x}}(t_i)$ as follows

$$\nabla_{\mathrm{i}} J[\tilde{\mathbf{x}}(t_1), \ldots, \tilde{\mathbf{x}}(t_N)] = \mathbf{B}^{-1}\left[\tilde{\mathbf{x}}(t_i) - \tilde{\mathbf{x}}_{\boldsymbol{g}}(t_i)\right] + \sum_{j=1}^{K} \mathbf{M}^{\mathbf{T}} \mathbf{H}^{\mathbf{T}} \boldsymbol{R}^{-1}\left[\boldsymbol{H}(\mathbf{x}(t_j)) - \boldsymbol{y}_j\right] + \nabla_{\mathrm{i}} J_{\mathrm{p}}$$

where $\mathbf{M}^{\mathbf{T}}$ is the adjoint of the forward model $\boldsymbol{M}_t$, as follows

$$\boldsymbol{M}_t(\tilde{\mathbf{x}} + \delta\tilde{\mathbf{x}}) = \boldsymbol{M}_t(\tilde{\mathbf{x}}) + \delta\tilde{\mathbf{x}} \frac{\partial \boldsymbol{M}_t}{\partial \tilde{\mathbf{x}}}$$

$$\mathbf{M}^{\mathbf{T}} = \left(\frac{\partial \boldsymbol{M}_t}{\partial \tilde{\mathbf{x}}}\right)^{T}$$

Similarly, $\mathbf{H}^{\mathrm{T}}$ is adjoint of the observation operator $\boldsymbol{H}$, as follows

$$\boldsymbol{H}(\mathbf{x} + \delta\mathbf{x}) = \boldsymbol{H}(\mathbf{x}) + \delta\mathbf{x} \frac{\partial \boldsymbol{H}}{\partial \mathbf{x}}$$

$$\mathbf{H}^{\mathbf{T}} = \left(\frac{\partial \boldsymbol{H}}{\partial \mathbf{x}}\right)^{T}$$

The adjoint model $\mathbf{M}^{\mathbf{T}}$ calculates the sensitivity of cost function J for emission mass $\tilde{\mathbf{x}}(t_1), \ldots, \tilde{\mathbf{x}}(t_N)$ from misfits between observation and forecast $\mathbf{H}^{\mathbf{T}} \boldsymbol{R}^{-1}[\boldsymbol{H}(\mathbf{x}(t_j)) - \boldsymbol{y}_j]$ in a model space at time t_j, including observation error as weight. Once we obtain a gradient of cost function $\nabla_{\mathrm{i}} J$, the iteration method can be performed to minimize the cost function. In this study, the limited-memory quasi-Newton (L-BFGS) algorithm is used as the iteration minimizing algorithm (Liu and Nocedal 1989). In Fig. 1, the flow of the overall system is shown.

Application to the 2016 Aso volcano eruption

We adopted the 4D-Var system for the 01:46 (JST) October 8, 2016 eruption of Aso volcano in Kyushu, Japan, which is an active volcano that JMA monitors with various instruments such as seismometers, tiltmeters and remote cameras. Most recently, several ash emissions (2003–2005) and volcanic gases and ash emissions (2014–2016) occurred (Miyabuchi et al. 2008; Marumoto et al. 2017). According to Ishii et al. (2018), in the October 2016 eruption, SO_2 emitted from the eruption reached an altitude of 13–14 km, and the ash and lapilli fall spread several kilometres, mainly to the northeast by the ambient wind. Furthermore, lapilli which fell approximately 4.5 km from the vent broke window panes, and lapilli which fell approximately 6.5 km away broke more than 1500 solar panels.

Observation used in the 4D-Var system

In this study, the input into the 4D-Var system is ash fall (including lapilli) and radar observations.

In the October 8, 2016 eruption, ash and lapilli fall spread to the northeast area of Aso volcano. Ash fall observations were performed from a few hours after the eruption by JMA-MOT (JMA Mobile Observation Team). However, in this experiment, it is assumed that observed ash fall was sedimented within 2 h after the eruption (i.e. 01:47–03:47 JST). Although we have no time series of ash fall observation, accounting for wind from aerological observation, etc., on the day, this assumption is sufficiently realistic. In addition to JMA-MOT field observations, JMA directly confirmed if ash had fallen or not by asking public offices (such as police stations) in the wider region. In this information,

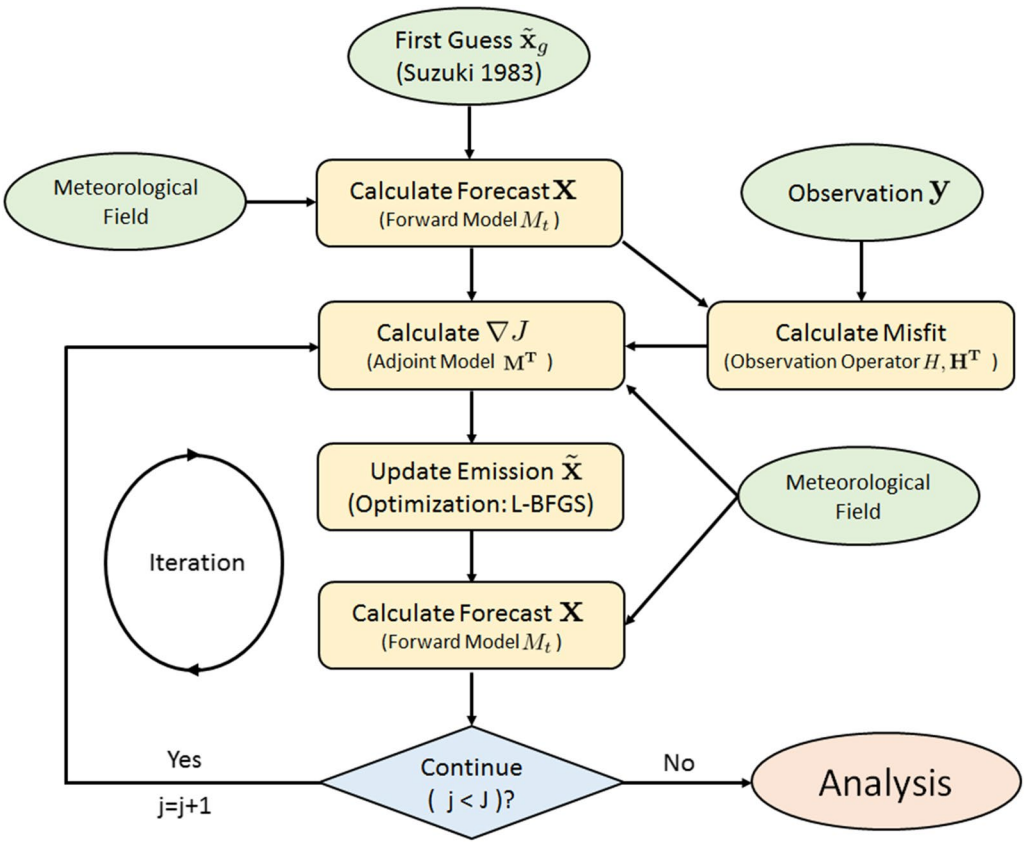

Fig. 1 Schematic showing 4D-Var iterative procedure in this study

un-quantitative values, such as "Ash fell but the amount is unknown" and "Lapilli is on the ground but the amount is unknown", are included. Therefore, for this result of asking public offices, reports of "No Ash Fall" were used as ash fall 0 (g/m^2) [including lapilli 0 (g/m^2)], but un-quantitative values such as "Ash fell but the amount is unknown" were not used in this experiment. We assumed that observation of "Ash Fall Only" includes "No Lapilli". Besides, the eruption plume was captured as radar echoes by JMA operational weather radars, and the top height of the plume was estimated about 12,000 m $\pm$ 687 m above sea level (Sato et al. 2018). In this study, radar observation which is input into the 4D-Var system assumes that there is no ash and lapilli above 13 km above sea level (in this study, radar data do not have a quantitative parameter in the eruption column).

Simulation settings and first guess

In this simulation, the spatial coordinate is a horizontal grid spacing of 0.01 degrees and a vertical grid spacing of 1 km. The area of calculation is 32.75–33.55 degrees for latitude and 130.95–131.75 degrees for longitude, and the surface—16 km for altitude. The time step is 1 s. The forecast time is 2 h from eruption (i.e. time of ash fall observation). Forecast variables are ash concentration of ϕ-scale -4 to $+4$ discretized to 20 bins. Each variable has density which is based on Wilson and Huang (1979) (Table 1). The emission mass profile is based on the emission source model Suzuki (1983). In this study, as a centre diameter d_m and standard deviation σ of log-normal distribution, we used $d_m = 0.25$ mm, $\sigma = 1.0$ based on Shimbori (2015). The start time of the eruption and duration of the eruption are 01:46 October 8, 2016 (JST) and 180 s from seismometer observation (Ishii et al. 2018). The vent is located at 32.8836N, 131.0969E. Total mass emission (i.e. eruption mass) for ash fall deposit (including lapilli-size crusts) is assumed as 1.8×10^8 kg from field survey (Miyabuchi et al. 2017). In this study, the meteorological field is the Meso Analysis of initial time 00, 03 and 06 JST to be interpolated linearly by the time and space. The background error covariance **B** assumes Gaussian statistics between distance

Table 1 List of parameters for classified ash particle size

Index	ϕ-scale	Density (kg/m^3)	D (mm)
1	− 4.00	1116	16.0000
2	− 3.58	1121	11.9501
3	− 3.16	1129	8.9253
4	− 2.74	1138	6.6661
5	− 2.32	1150	4.9788
6	− 1.89	1166	3.7185
7	− 1.47	1187	2.7773
8	− 1.05	1214	2.0743
9	− 0.63	1249	1.5493
10	− 0.21	1292	1.1571
11	0.21	1344	0.8642
12	0.63	1408	0.6455
13	1.05	1481	0.4821
14	1.47	1564	0.3600
15	1.89	1655	0.2689
16	2.32	1749	0.2009
17	2.74	1843	0.1500
18	3.16	1933	0.1120
19	3.58	2017	0.0837
20	4.00	2090	0.0625

and correlation for vertical distribution, and between distance and correlation for size distribution. The element of **B** is as follows.

$$B(z_i, z_j; \phi_n, \phi_m) = B_0 \exp\left[-\frac{(z_i - z_j)^2}{\sigma_z^2}\right] \times \exp\left[-\frac{(\phi_n - \phi_m)^2}{\sigma_\phi^2}\right]$$

where z_i, z_j are altitudes which are discretized and ϕ_n, ϕ_m are ash particle diameters which are discretized.

The dump coefficient of Gaussian σ_z and σ_ϕ is, respectively, 500 m and 1ϕ, and B_0 is 10 g/m^3. It is assumed that the observation error covariance is diagonal. Error of ash fall observation is 10% of the measured value, and error of radar observation is 10^{-3} g/m^3.

As mentioned above, the penalty term is used to avoid negative emission mass. The parameter μ in the penalty term needs to be sufficiently large. However, a too large value leads that a penalty term is too dominant in the cost function, while a too small value leads negative mass emission. As a result of trying some values, we chose $\mu = 20{,}000$ (m^6/g^2).

Simulation results

Figure 2 shows that the ash fall simulation results with three hundred 4D-Var iteration steps, updating the first guess every 20 steps, are shown in Fig. 2. The ash fall forecast with the 4D-Var system is closer to observation than that with no 4D-Var. Especially, the main axis of ash fall moved southward which is more consistent with observation, and in the west and south of the main axis of ash fall, we can see an improvement of ash fall forecast. That is, in the result of no assimilation, the ash fall is overestimated clearly around the northwest and south ash fall area of the main axis; however, with 4D-Var this is improved. As expected, these improvements were due to ash fall observations.

The emission mass of the first guess and analysis, and corrections by the 4D-Var system (called "analysis increment" or "increment") are shown in Fig. 3. The overestimation of ash fall, which is forecast from the first guess to be compared to the ash fall observations in the west area, decreases emission mass of fine ash from low altitude (surface—5000 m, $0 \le \phi \le 3$). Besides, the difference between ash fall observations (with no ash) and ash fall forecast with no 4D-Var (Fig. 2a) in the south area of the main axis decreases emission mass at high altitude and coarse ash (surface—10,000 m, $-4 \le \phi \le -1$). In addition, there are positive increment areas at "7000–12,000 m of altitude around $0 \le \phi \le 1$". This positive increment is due to underestimations of forecast with no 4D-Var around the main axis from observation (around the area of ash fall observation 109 g/m^2, 183 g/m^2, see Fig. 2a).

Figure 4 is a plot between observation and forecast for ash fall. It shows that the ash fall forecast calculated from the emission mass with the 4D-Var system is better than that with no 4D-Var. Therefore, this improvement of forecast suggests that ash emission mass from the eruption column was improved by the 4D-Var system and observation. However, for some ash fall observations with large amounts (> 500 g/m^2, i.e. observation close to the vent), the ash fall forecast with 4D-var was worse than that from the first guess (small window in Fig. 4). This implies that phenomena close to the vent, including complex transport and depositional processes with a huge variation of ash fall locally, cannot be treated properly in this system.

Discussion

Generally, because ash particles from each altitude and in each size fall at a variety of locations, an appropriate spatial arrangement of ash fall observation is needed for the accurate estimation of emission mass. Actually, in this case, inaccuracy from a lack of ash fall observation appeared in the estimation of emission mass by the

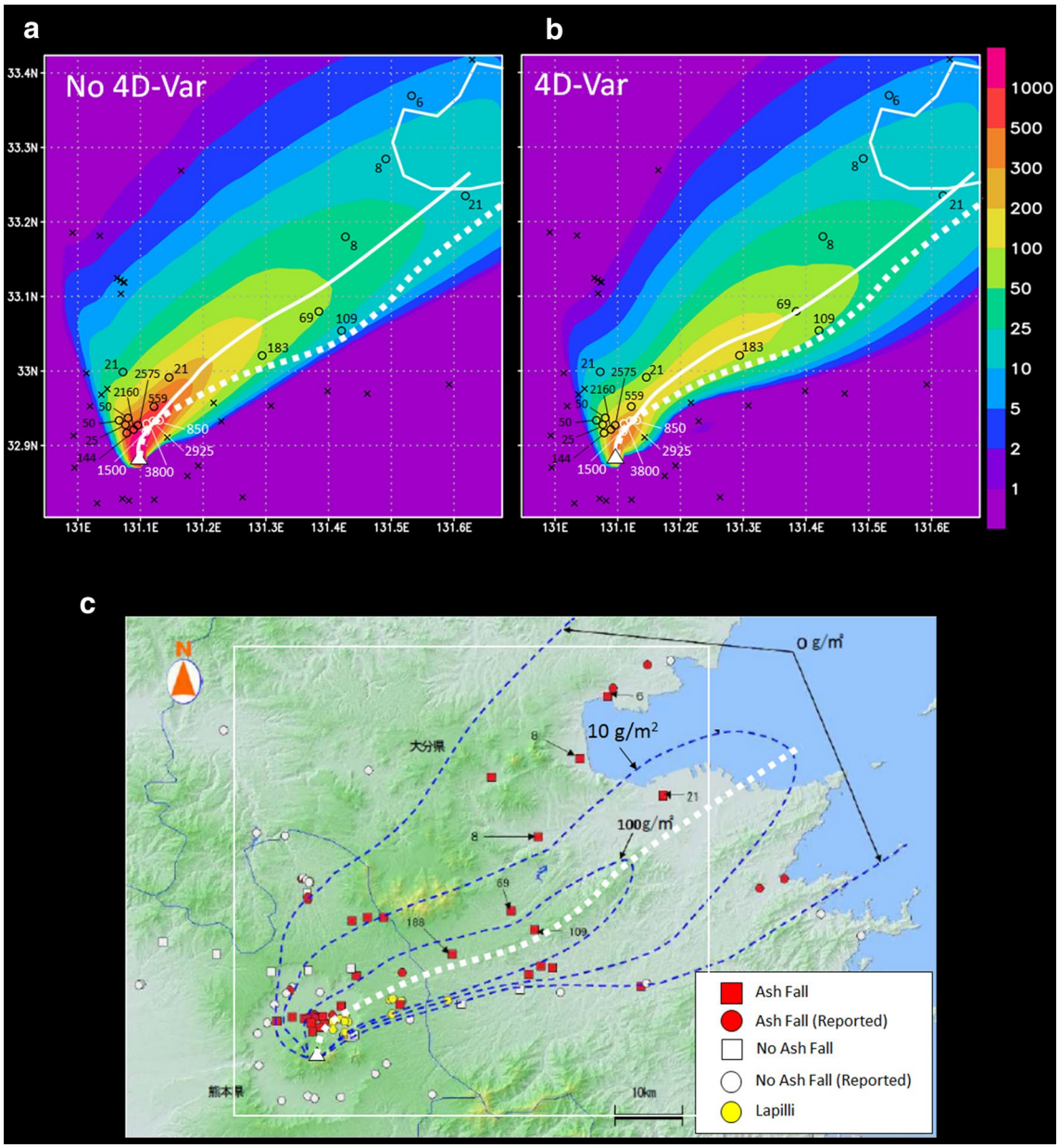

Fig. 2 **a** Ash fall forecast without 4D-Var. **b** Ash fall forecast with 4D-Var. **c** Ash fall observation [Regional Volcanic Observation and Warning Center, Fukuoka Regional Headquarters, JMA (2018) (minor postscripts were added by the author)]. The white triangle is plotted at the location of Aso volcano for all figures. In the left and centre figures, black cross-marks are "No Ash Fall and No Lapilli Fall", black circles are "Ash Fall (g/m^2), No Lapilli Fall", and white circles are "ash fall and lapilli fall (g/m^2)". White solid lines in the left and centre figures are the main axis of ash fall forecast. The white dotted line is the main axis estimated from observation

4D-Var system. In Fig. 3, there is no correction for high altitude and fine ash (above 6000 m, $2 \leq \phi \leq 4$). Typically, fine ash is blown a long distance. Especially, fine ash particles emitted from high altitude reach several hundreds to several thousands of kilometres away. Therefore, in order to correct fine ash emission from high altitude, ash observations in distant locations are needed.

However, in this study, we only have ash fall observations in the region of Aso volcano. (Observation points are shown in Fig. 2.) For this reason, fine ash emission from high altitude of the first guess could not be corrected by ash fall observations. That is, the analysis value is almost the value of the first guess in the region for high altitude and fine ash. Except for large eruptions,

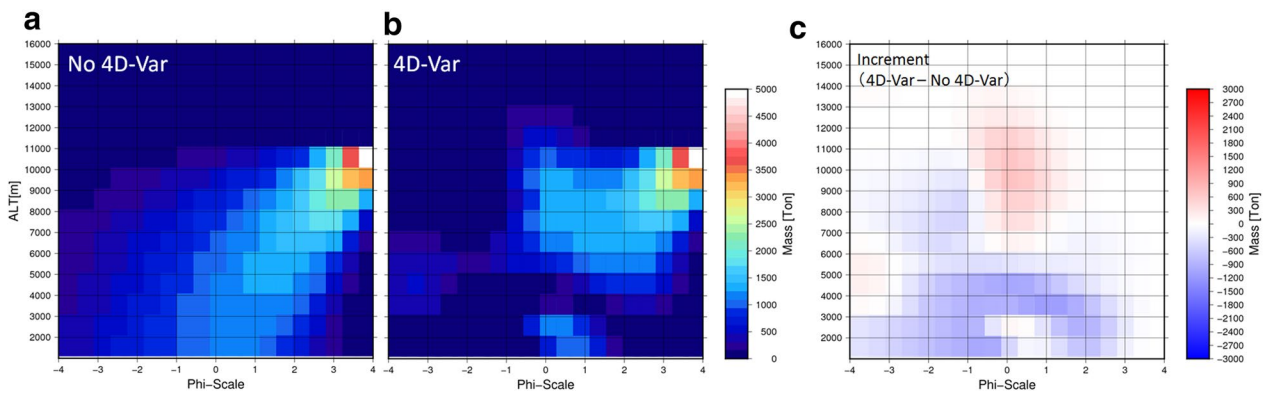

Fig. 3 Ash emission mass from eruption plumes. **a** First guess based on Suzuki (1983). **b** Analysis (corrected first guess by 4D-Var). **c** Analysis increment (analysis—first guess)

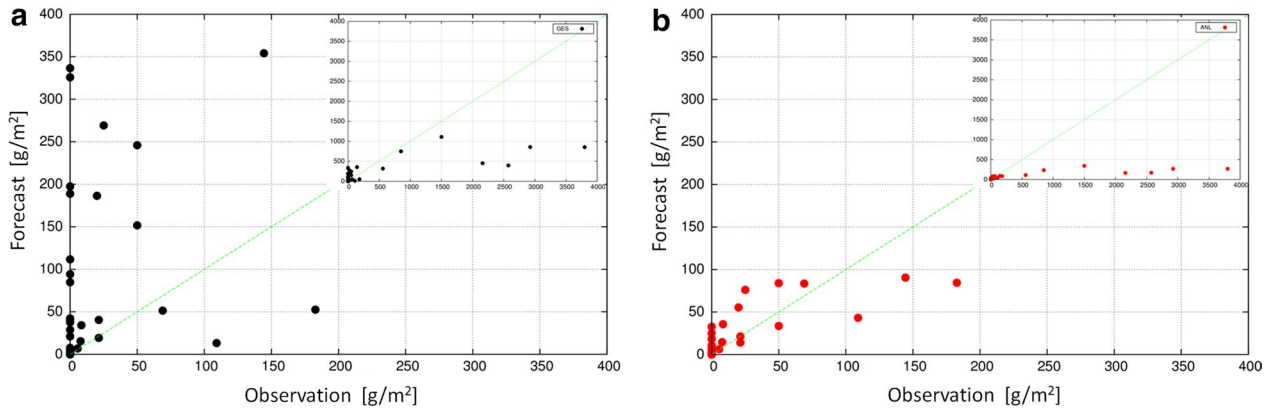

Fig. 4 Comparison between observation and simulation for ash fall and lapilli. **a** Without 4D-Var. **b** With 4D-Var. Small windows in both figures are enlargements of large regions (0–4000 g/m^2)

we cannot obtain quantitative ash fall observations several hundreds to several thousands of kilometres away because often the ash fall amount is too small to be measured accurately and to be represented locally because of dispersion over a long time, that is, more than 1 day. In this case, ash particles could only be identified by microscopic analysis at the Okayama Meteorological Observatory, over 300 km from Aso volcano (done by Dr. Yaguchi, who reported it). Therefore, when the ash fall amount is too small, it is difficult to obtain accurate and local representative observation values, so it is not expected that a 4D-Var system with ash fall observation can correct emission mass of fine ash from high altitude. For example, although the eruption mass which is the sum of emission mass from the eruption column could be estimated to be 1.32×10^8 kg, it should be noted that this value includes some errors associated with a lack of observation such as this case. For a solution to this problem of fine particles from high altitude, other observations such as volcanic ash mass loading from satellite observation (e.g. Bessho et al. 2016) are necessary. The volcanic ash mass loading from satellite observation provides the amount of fine ash in the atmosphere before fall and a few hours after eruption. In addition, in this study, ash fall observation includes only the amount of ash (and lapilli) and does not include size distribution or a time series of ash fall. For example, additional observation including these, such as PARSIVEL (e.g. Iriyama 2018), could be expected to improve the accuracy of estimation. In the 4D-Var system, it is necessary to develop an observation operator $\boldsymbol{H}(\mathbf{x})$, its tangent linear $\frac{\partial \boldsymbol{H}}{\partial \mathbf{x}}$ and its adjoint $\mathbf{H}^{\mathrm{T}}$ to introduce new observations. The 4D-Var system can treat a variety of observations simultaneously by the development of the observation operators. This scalability for additional observation is the most significant point for the 4D-Var system.

It also should be noted that the emission mass estimated by the 4D-Var system includes also errors

associated with uncertainty of the numerical model. In this case, even if ash fall observation is used, ash fall observation close to the vent could not be reproduced by the 4D-Var system because of model uncertainties such as complex transport and depositional processes with a huge variation of ash fall locally. For the solution to this problem, the model uncertainties will need to be reduced. One solution may be a high-resolution model including complex processes such as entrainment of ambient air into eruption clouds by turbulent mixing (e.g. Suzuki et al. 2005).

Conclusion and future work

In this study, in order to obtain emission mass from the eruption column for each altitude and each size of ash particles, we developed a data assimilation system based on 4D-Var. This system was applied to the Aso volcano eruption at 01:46 on October 8, 2016, and observation for the data assimilation system is the ash fall (including lapilli) and meteorological radar. Except for fine ash from high altitude, the first guess was corrected by ash fall observation in the data assimilation system. Using the corrected first guess (i.e. analysis), the numerical model led to an ash fall forecast which is more consistent with ash fall observations than the first guess.

However, the 4D-Var data assimilation system did not correct emission mass of fine ash from high altitude because the ash fall observation in the region of the volcano does not have sensitivity for fine ash from high altitude, as it does not fall in the region of the volcano. In order to correct fine ash from high altitude, it is necessary to have other observations such as mass loading from satellites.

In this study, we developed a novel data assimilation system for volcanic ash. There are many unknown parameters such as σ_z, σ_ϕ and B_0 background error covariance $\mathbf{B}$, error of ash fall observation in the observation error covariance $\mathbf{R}$, and the penalty term factor μ. We could not check these parameters sufficiently. In addition, ash fall close to vent also could not be reproduced by this system. The solution to this problem may be the use of high-resolution models including complex processes. From the above, a lack of understanding remains in the interpretation of the emission mass estimated by the 4D-Var system. Therefore, it is should be noted that eruption mass 1.32×10^8 kg estimated by 4D-Var system includes some errors. Nevertheless, the ash emission mass estimated by the 4D-Var system led to an ash fall forecast which is much more consistent with ash fall observation than that with no 4D-Var, except for the area close to the vent.

Recently, quantitative retrieval techniques using remote sensing have been developed. For example, Marzano et al. (2013) developed quantitative retrieval techniques inside eruption columns based on weather radar. Comparison between the 4D-Var estimate and radar observation for an eruption column may reveal disadvantages and validate/improve each scheme.

Abbreviations

JMA: Japan Meteorological Agency; 4D-Var: four-dimensional variational method.

Authors' contributions

KI developed the data assimilation system and applied it to the October 8, 2016 Aso volcano eruption in Japan. The author read and approved the final manuscript.

Acknowledgements

We thank the two anonymous reviewers for their useful comments and suggestions.

Competing interests

The author declares that he has no competing interests.

Consent for publication

Not applicable.

Ethics approval and consent to participate

Not applicable.

Funding

None.

Publisher's Note

Received: 12 September 2018 Accepted: 29 November 2018
Published online: 19 December 2018

References

Bessho K et al (2016) An introduction to Himawari-8/9—Japan's new-generation geostationary meteorological satellites. J Meteorol Soc Jpn 94:151–183. https://doi.org/10.2151/jmsj.2016-009

Bonadonna C et al (2005) Probabilistic modeling of tephra dispersal: hazard assessment of a multiphase rhyolitic eruption at Tarawera, New Zealand. J Geophys Res Solid Earth 110:B03203. https://doi.org/10.1029/2003JB002896

Folch A (2012) A review of tephra transport and dispersal models: evolution, current status, and future perspectives. J Volcanol Geotherm Res 235–236:96–115. https://doi.org/10.1016/j.jvolgeores.2012.05.020

Iriyama Y et al (2018) In situ observation of falling ash by using PARSIVEL disdrometer during the 2018 eruption at Shinmoe-dake volcano, Japan. Abstract of cities on volcanoes. https://www.citiesonvolcanoes10.com/wp-content/uploads/2018/08/COV10-2018-Conference_Program.pdf. Accessed 11 Oct 2018

Ishii K et al (2018) Using Himawari-8, estimation of SO_2 cloud altitude at Aso volcano eruption, on October 8, 2016. Earth Planets Space 70:19. https://doi.org/10.1186/s40623-018-0793-9

Japan Meteorological Agency (2013) Outline of the operational numerical weather prediction at the Japan Meteorological Agency, pp 43–61. http://www.jma.go.jp/jma/jma-eng/jma-center/nwp/outline2013-nwp/index.htm. Accessed 19 July 2017

Kalnay E (2002) Atmospheric modeling, data assimilation and predictability. Cambridge University Press, Cambridge

Klawonn M et al (2012) Novel inversion approach to constrain plume sedimentation from tephra deposit data: application to the 17 June 1996 eruption of Ruapehu volcano, New Zealand. J Geophys Res Solid Earth. https://doi.org/10.1029/2011jb008767

Koren B (1993) A robust upwind discretization method for advection, diffusion and source terms. CWI technical report NM-R 9308, pp 1–22. http://oai.cwi.nl/oai/asset/5293/05293D.pdf. Accessed 10 Aug 2018

Liu CD, Nocedal J (1989) On the limited memory BFGS method for large-scale optimization. Math Progr 45:503–528. https://doi.org/10.1007/BF01589116

Mannen K (2014) Particle segregation of an eruption plume as revealed by a comprehensive analysis of tephra dispersal: theory and application. J Volcanol Geotherm Res 284:61–78. https://doi.org/10.1016/j.jvolgeores.2014.07.009

Marumoto K et al (2017) Collateral variations between the concentrations of mercury and other water soluble ions in volcanic ash samples and volcanic activity during the 2014–2016 eruptive episodes at Aso volcano, Japan. J Volcanol Geotherm Res 341:149–157. https://doi.org/10.1016/j.jvolgeores.2017.05.022

Marzano FS et al (2013) Inside volcanic clouds: remote sensing of ash plumes using microwave weather radars. Bull Am Meteorol Soc 94:1567–1586. https://doi.org/10.1175/BAMS-D-11-00160.1

Miyabuchi Y et al (2017) The October 7–8, 2016 eruptions of Nakadake Crater, Aso Volcano, Japan and their deposits. Abstract of Japan Geoscience Union—American Geoscience Union joint meeting 2017: SVC47-11. https://confit.atlas.jp/guide/event-img/jpguagu2017/SVC47-11/public/pdf?type=in. Accessed 10 Aug 2018

Miyabuchi Y et al (2008) Geological constraints on the 2003–2005 ash emissions from the Nakadake crater lake, Aso Volcano, Japan. J Volcanol Geotherm Res 178:169–183. https://doi.org/10.1016/j.jvolgeores.2008.06.025

Parrish FD, Derber CJ (1992) The National Meteorological Center's spectral statistical-interpolation analysis system. Mon Weather Rev 120:1747–1763. https://doi.org/10.1175/1520-0493(1992)120%3c1747:TNMCSS%3e2.0.CO;2

Regional Volcanic Observation and Warning Center, Fukuoka Regional Headquarters, JMA (2018) Volcanic activity before and after the explosive eruption of Asosan on October 8, 2016. Coordinating Committee for Prediction of Volcanic Eruptions (CCPVE) 126, pp 144–174. https://www.data.jma.go.jp/svd/vois/data/tokyo/STOCK/kaisetsu/CCPVE/Report/126/kaiho_126_25.pdf. Accessed 10 Aug 2018

Sato E et al (2018) Aso volcano eruption on October 8, 2016, observed by weather radars. Earth Planets Space 70:105. https://doi.org/10.1186/s40623-018-0879-4

Shimbori T (2015) Tephra fall prediction by numerical simulation. Earozoru Kenkyu 30(3):168–176. https://doi.org/10.11203/jar.30.168 **(in Japanese, with English abstract and captions)**

Shimbori T et al (2010) Quantitative tephra fall prediction with the JMA mesoscale tracer transport model for volcanic ash: a case study of the eruption at Asama volcano in 2009. Pap Meteorol Geophys 61:13–29. https://doi.org/10.2467/mripapers.61.13 **(in Japanese, with English abstract and captions)**

Suzuki T (1983) A theoretical model for dispersion of tephra. In: Shimozuru D, Yokoyama I (eds) Arc volcanism, physics and tectonics. Terra Scientific Publishing Company, Tokyo, pp 95–113

Suzuki Y, Koyaguchi T, Ogawa M, Hachisu I (2005) A numerical study of turbulent mixing in eruption clouds using a three-dimensional fluid dynamics model. J Geophys Res 110:B08201. https://doi.org/10.1029/2004JB003460

Wicker JL, Skamarock CW (2002) Time-splitting methods for elastic models using forward time schemes. Mon Weather Rev 130:2088–2097. https://doi.org/10.1175/1520-0493(2002)130%3c2088:TSMFEM%3e2.0.CO;2

Wilson L, Huang TC (1979) The influence of shape on the atmospheric setting velocity of volcanic ash particles. Earth Planet Sci Lett 44:311–324. https://doi.org/10.1016/0012-821X(79)90179-1

World Meteorological Organization (2001) WMO technical progress report on the global data-processing and forecasting system (GDPFS) and numerical weather prediction (NWP) research. https://www.wmo.int/pages/prog/www/DPFS/ProgressReports/. Accessed 10 Aug 2018